Title:

Chain-Growth Synthesis of Extensively Cross-Conjugated Polyenes via Strained [3]Cumulenes

Authors: Zi-Yuan Wang[1], Yi-Ze Xu[1], Zhanpeng Cui[2], Jia-Yu Lu[1], Yu-Qing Zheng[2]*, Rong Zhu[1]*

Affiliations: [1]Beijing National Laboratory for Molecular Sciences (BNLMS), Key Laboratory of Bioorganic Chemistry and Molecular Engineering of Ministry of Education, College of Chemistry and Molecular Engineering, Peking University, Beijing, China.

[2]National Key Laboratory of Advanced Micro and Nano Manufacture Technology; Beijing Advanced Innovation Center for Integrated Circuits, School of Integrated Circuits, Peking University, Beijing 100871, China.

*Corresponding authors. Email: rongzhu@pku.edu.cn (R.Z.); zhengyq@pku.edu.cn (Y.Q.Z.).

One Sentence Summary (120/125 characters):

Chain-growth polymerization of strained cumulenes enables extensively cross-conjugated polyenes of unprecedented length.

Abstract (104/125 words):

For years, polyenes with an extensively cross-conjugated backbone have fascinated chemists by their unique opto-electronic properties and reactivities, but so far only short oligomers (≤ 12 vinylene units) are available through multi-step assembly of vinylic building blocks. Here, we report a single-step chain-growth approach that streamlines the synthesis of cross-conjugated polyenes with up to 86 consecutive vinylene units averaged per chain and well-defined end groups. This method highlights a key interaction between an organocopper species with a strained [3]cumulene, unlocking a previously unknown 2,3-polymerization pathway. The resulting polyenes display decent two-photon-absorption capacity without compromising visible transparency, facilitating visible range two-photon lithography with sub-diffraction-limit resolution.

Main Text:

The conjugation topology of a π-conjugated scaffold can profoundly impact its optical and electronic properties (Fig. 1A).(*1-2*) Polymers with an extended linearly-conjugated backbone allows for effective delocalization and have been the subject of most studies. Their counterpart, cross-conjugated polymers, featuring branched π-groups and attenuated delocalization along the main chain, have historically received less attention.(*3-6*) However, it is recently realized that unique properties can arise from such an "interrupted" electronic communication. For instance, cross-conjugation has been associated with the destructive quantum interference phenomenon in single-molecule electronics, and therefore affords large on–off ratios.(*7-9*) In the field of organic nonlinear optics, and in particular two-photon absorption (TPA) materials, Tykwinski showed that helical cross-conjugated oligomers are promising candidates to circumvent the "transparency-nonlinearity trade-off" found in linearly-conjugated materials, due to their richness in π-electrons and length-independent absorption-edge.(*10-13)*

Despite significant synthetic advances, the currently available cross-conjugated polymers are virtually "mixed" in terms of linearly- and cross-conjugated units in the backbones.(*14-21*) In this regard, a prototypical linear polyene with the most extensive cross-conjugation possible, namely a poly(1,1-vinylene)-type framework, has been highly desired yet elusive.(*22-23*) Some works have tackled oligomers in this class (Fig. 1B). The parent structure, also known as dendralenes, has been obtained by Sherburn via multiple cross-coupling reactions with the longest record of 12 vinylene units.(*24*) Dong and Liu developed an iterative alkenylidene homologation strategy through a novel S_NV pathway and achieved up to a pentamer.(*25*) Whereas these elegant step-growth methods afford precise short oligomers, extending the chemistry to higher ones (n >

12) or even polymers is likely challenging, due to the limited reaction efficiency and decreasing intermediate stability over steps.

Rather than stepwise assembling vinylic building blocks, we sought a chain-growth strategy based on cumulenes. Three addition-polymerization modes can be conceived for a [3]cumulene (Fig. 1C). We have previously realized the 1,4-polymerization mode by an organocopper-mediated process, which yields an alkyne backbone.(*26-28*) It was envisioned that, if this established regioselectivity could be overwhelmed by a 2,3-selective addition, a streamlined synthesis of poly(1,1-vinylene) structure would become possible. Although this polymerization mode is unknown, we drew inspirations from literature regarding highly strained [3]cumulenes. (*29-31*) Their lowest unoccupied molecular orbitals (LUMO) are significantly altered by geometric constrain, leading to preferential reaction at the central in-plane olefin. Taking this concept, cycloaddition and nucleophilic addition have been demonstrated.(*31-32*) In contrast, reactions via interacting with an organometallic species remain largely unexplored.(*33*)

Here we report the 2,3-polymerization of strained cyclic [3]cumulenes towards extensively cross-conjugated polyenes (Fig. 1D). Through an organocopper-mediated chain-growth process, we are able to achieve purely cross-conjugated backbones with a record-breaking length (i.e. poly(1,2,3-cyclohexatriene)s (**PCHTs**), up to 86 vinylene units by average) and well-defined end groups. Spectroscopic analysis, computational modeling, and analogy to known foldamer systems suggest helical conformations for **PCHTs**, which brings decent TPA ability along with visible transparency. While being thermally stable, this cross-conjugated polyene backbone naturally responds to photo-excitation and generates reactive radicals. Combining these unique properties, **PCHTs** as a new TPA photoinitiator class successfully enable visible range two-photon lithography (TPL) with sub-diffraction-limit resolution.

We commenced our study by evaluating the organocopper-mediated polymerization of a Kobayashi silyl triflate (**M1**), which can be activated by fluorides to release the corresponding 1,2,3-cyclohexatriene in situ (Fig. 2A).(*31*, *34*) Since the dendralene-type structures are well-known to undergo Diels-Alder reactions, a quaternary substitution is added to the monomer structure to sterically inhibit the product decomposition and meanwhile enhance the solubility.(*35*) In tetrahydrofuran (THF) at 60 °C, using cuprous cyanide (CuCN) as an initiator, the target polymer **PCHT-1** was obtained in 65% yield (entry 1, $M_{n,\,GPC}$ = 3.0 kDa, $Đ$ = 1.9, degree of polymerization (DP) ~ 29). No polymer was detected in the absence of a Cu(I) initiator, and a complex mixture was formed including various cycloaddition products (entry 2). A higher molecular weight (MW) can be achieved by elevating the **M1**/CuCN feed ratio at the expense of diminished yield (entry 3, $M_{n,\,GPC}$ = 4.3 kDa, $Đ$ = 1.6). Alternative organocopper and -palladium complexes were found to promote the polymerization, albeit with inferior yields and MW (entry 4-7). The addition of a phosphine led to decreased MW, presumably due to competing phosphine-initiated oligomerization (entry 8).(*36*) A super excess of cesium fluoride and 18-crown-6 was necessary for efficient activation (entry 9-10). Low MW was obtained by either diluting the reaction, using alternative solvents, or leaving out the 4Å molecular sieves (MS), which scavenges the trace moisture that could terminate the putative organocopper chain end (entry 11-14).

A brief survey of the monomer scope was then performed (Fig. 2B). Flexible side chains improved the MW by further adding solubility (**PCHT-2**). Allyl ethers were well tolerated, which could be used as a post-modification handle or removed to reveal hydroxyl groups (**PCHT-3**). As the distal quaternary carbon has minimal effect on the propagation regiochemistry, these polymers contain mixed head/tail connectivity. We were able to extend this chemistry to obtain a poly(1,2,3-

cycloheptatriene) (**PCHPT**). However, further increasing the ring size failed to produce the target polymer in substantial quantities. When an aryl substituent is introduced on the cyclic cumulene motif, sluggish propagation was observed, which could be attributable to severe steric hinderance (**PCHT-4**, DP ~ 7).

Extensive characterizations were performed to establish the backbone structure of **PCHTs**. Trimer **CHT-1$_3$** was independently synthesized and used as a model. As shown in Fig. 3A and 3B, ^{1}H and ^{13}C NMR spectra of **PCHT-1** are in good agreement with those of **CHT-1$_3$** with apparent peak-broadening. A heteronuclear single quantum coherence (HSQC) experiment was used to establish the C-H bond connectivity (Fig. 3C). The exclusive 2,3-regioselectivity is validated by the absence of acetylenic carbon and propargylic proton signals.

To assess the repeating units and end groups, we performed matrix-assisted laser desorption/ionization time-of-flight (MALDI-TOF) mass spectroscopic analysis on a sample of moderate-MW **PCHT-2** (CuCN-initiated, $M_{n,GPC}$ = 3.5 kDa). Correct peak spacings of m/z = 194.1 were observed (Fig. 3D). A cyano group at the α end and an end-capping H can be assigned, which is consistent with a chain-growth process initiated by CuCN and terminated by protonation. The GPC-assigned DP (~18) lies reasonably close to that estimated by mass spectroscopy (~23), which corresponds to 46 vinylenes in average. Thus, it can be inferred that with the higher MW sample of the same polymer shown in Fig. 2B ($M_{n,\,gpc}$ = 6.6 kDa), by average a remarkable 86 consecutive vinylenes have been assembled in a row. This may be considered a new record for dendralene-type molecules.(*24*)

Density functional theory (DFT) calculations were next employed to provide further insights into the polymerization mechanism (Fig. 3E). The coordination of the in-plane π-bond of 1,2,3-cyclohexatriene to a Cu(I) center is strongly exothermic because of the favored d-π* back-

bonding (ΔH = -33.7 kcal/mol). The resulting π-complex **Int-1** could slowly undergo migratory insertion (**TS-1**, $\Delta G^{\ddagger}$ = 25.2 kcal/mol) to form an alkenyl Cu(I) species **Int-2**, thereby completing the initiation process. Subsequently, the propagation could involve a similar coordination-insertion sequence via **Int-3**, which regenerates the alkenyl Cu(I) chain end **Int-4**. The high affinity of 1,2,3-cyclohexatriene to Cu(I) is likely the key to enable efficient polymerization of such a fleeting intermediate. We noticed that the migratory insertion of **Int-3** is much more facile (**TS-2**, $\Delta G^{\ddagger}$ = 13.1 kcal/mol). Hence, the slow initiation and fast propagation lead to an uncontrolled chain-growth process. On the other hand, insertion across the out-of-plane π-bond was found prohibitively high-barrier (Fig. S20), which is consistent with the exclusive 2,3-selective polymerization observed.

With the structures of **PCHTs** established, we set out to evaluate their optical properties. The absorption spectra of **PCHT-1** of different MWs ($M_{n,GPC}$ = 1.0, 2.2 kDa) closely resemble that of **CHT-1$_3$** (Fig 4A). As the molecules get longer, the molar extinction coefficients steadily increase at the maximum absorption (λ_{max} ~225 nm), which can be ascribed to the individual 1,3-butadiene repeating units.(*24*) Meanwhile, the transparency in the visible range is mostly preserved, which is characteristic of cross-conjugated systems because of their attenuated long-range π-delocalization. **PCHTs** could adopt either a *cisoid* or *transoid* conformation. As shown by modeling the oligomers, either a "closed" or "open" helical structure could be formed (Fig. 4B), which is reminiscent of its aromatic analog, oligo(*o*-phenylene) foldamers.(*37-38*) Time-dependent (TD) DFT calculation was performed on a trimer and a hexamer, respectively (Fig. 4C). The low-energy transitions of the more twisted *cisoid* conformer are essentially symmetry-forbidden and length-independent. In contrast, the less twisted *transoid* conformer would display

longer-wavelength absorptions that become progressively red-shifted upon chain extension. Experimentally, this conformational isomerism might be reflected by a shoulder absorption observed at ~275 nm for **PCHT-1**.(*39*) The length-independent λ_{max} and absorption edge of **PCHT-1** suggests it likely contains more *cisoid* conformers, which could make it spatially compact with a high π-electron density and thus potentially TPA-enabling.

In contrast to the parent dendralenes, **PCHT-1** is thermally stable up to 200 ℃ (Fig. S15). Such remarkable stability can be attributable to the allylic quaternary substitution that inhibits potential Diels-Alder and aerobic oxidation reactions. On the other hand, photo-generated carbon radical species from **PCHT-1** were readily detected by electron paramagnetic resonance (EPR) spectroscopy (Fig. S30), which can be trapped by 5,5-dimethyl-1-pyrroline *N*-oxide (DMPO) in the presence of sodium ascorbate to eliminate potential oxygen-based radical adducts (Fig. 4D).(*40*) To understand this photochemical reactivity, TD-DFT calculation was conducted using **CHT_3** as a model. The S_1 state of **CHT_3** contains a substantial diradical character, which is accompanied by apparent co-planarization of two adjacent butadiene fragments (Fig. 4E, dihedral angle 49° for S_0 and 17° for S_1). Indeed, **$CHT\text{-}1_3$** in dilute solution rapidly respond to UV-irradiation by self-polymerization. Therefore, the extensive cross-conjugated backbone could provide **PCHTs** with a built-in photoinitiator function.

As an emerging advanced nanofabrication technology enabling sub-diffraction-limit resolution, two-photon lithography (TPL) relies on photoinitiators with good TPA properties.(*41-42*) In conventional linearly-conjugated molecules, larger TPA can be obtained by increasing the conjugation length and the extent of symmetric charge transfer.(*43*) However, this is accompanied by strong one-photon absorption in the visible range. As a result, TPL is typically performed using near-infrared lasers, despite the Rayleigh criterion suggests that visible lasers can achieve smaller

focal volumes and hence even higher resolutions.(*44*) To this, visible-transparent cross-conjugated molecules with a high spatial density of polarizable π-electrons could offer an alternative.(*12*) Indeed, **PCHT-1** was evaluated by open-aperture Z-scan technique, giving a TPA cross-section (δ) of 128 GM (10^{-50} cm^4 s/photon) at 650 nm while showing no one-photon absorption at this wavelength. Since δ depends on the size of the molecule, a MW-normalized number (δ/MW) is computed to be 58 GM/kDa. This is comparable to some state-of-art visible-range TPA initiators (46 GM/kDa for 7-diethylamino-3-thenoylcoumarin and 67 GM/kDa for 2,4-bis(trichloromethyl)-6-(4-methoxystyryl)-1,3,5-triazine, at 780 nm).(*45*) Moreover, the incorporation of an aminoaryl group on the 1,3-diene moiety was found to further boost the normalized TPA significantly (**PCHT-4**, 330 GM/kDa).

The results of TPA measurement and photoinduced radical generation paved the way to test **PCHT** as a new photoinitiator class for visible-range TPL. As a proof-of-concept study, a photoresist was formulated by mixing a cross-linkable monomer, namely pentaerythritol tetraacrylate (PETA) with **PCHT-1** (Fig. 4F). Submicron features were printed using 535 nm femtosecond laser direct writing, where the linear absorption of **PCHT-1** is negligible. To our delight, using 0.3 wt% **PCHT-1**, a parallel line array with a line width of 236 nm was obtained at a laser power of 10.0 mW and printing speed of 250 μm/s (Fig. 4G). More complex microstructures can also be created (Fig. 4H). Single-photon control experiments (535 nm continuous-wave laser with 100 mW power) gave no detectable polymerization, substantiating the necessity of TPA process (Fig. S35). This is also consistent with the sub-diffraction-limit resolution observed. The correlation between the feature size and laser power at different printing speeds is shown in Fig. 4I, indicating that the line width can be reduced by either smaller laser power or faster printing.

Built on this preliminary result, we envision that a reduced feature size could be realized by further solubility tuning and structure engineering of the **PCHT** skeleton.

In conclusion, a single-step chain-growth approach to extensively cross-conjugated polyenes of a record-breaking length is developed. This method highlights a key interaction between an organocopper species with a strained [3]cumulene, thereby unlocking a previously unknown 2,3-polymerization pathway. The present work opens up fresh opportunities for a deeper understanding of cross-conjugated systems and their associated applications, such as in visible-range two-photon lithography.

References and Notes

1. M. B. Nielsen, F. Diederich, Conjugated oligoenynes based on the diethynylethene unit. *Chem. Rev.* **105**, 1837–1868 (2005). doi: 10.1021/cr9903353
2. M. Gholami, R. R. Tykwinski, Oligomeric and polymeric systems with a cross-conjugated π-framework. *Chem. Rev.* **106**, 4997–5027 (2006). doi: 10.1021/cr0505573
3. P. A. Limacher, H. P. Lüthi, Cross conjugation. *Wires Comput. Mol. Sci.* **1**, 477–647 (2011). doi: 10.1002/wcms.16
4. E. G. Mackay, M. S. Sherburn, Demystifying the dendralenes. *Pure Appl. Chem.* **85**, 1227–1239 (2013). doi: 10.1351/PAC-CON-13-02-04
5. J. N. Wilson, P. M. Windscheif, U. Evans, M. L. Myrick, U. H. F. Bunz, Band gap engineering of poly(*p*-phenyleneethynylene)s: cross-conjugated PPE-PPV hybrids. *Macromolecules* **35**, 8681–8683 (2002). doi: 10.1021/ma025616i
6. T. P. Voortman, D. Bartesaghi, L. J. A. Koster, R. C. Chiech, Cross-conjugated n-dopable aromatic polyketone. *Macromolecules* **48**, 7007–7014 (2015). doi: 10.1021/ja8044053
7. G. C. Solomon, D. Q. Andrews, R. H. Goldsmith, T. Hansen, M. R. Wasielewski, R. P. Van Duyne, M. A. Ratner, Quantum interference in acyclic systems: conductance of cross-conjugated molecules. *J. Am. Chem. Soc.* **130**, 17301–17308 (2008). doi: 10.1021/ja8044053
8. C. M. Guédon, H. Valkenier, T. Markussen, K. S. Thygesen, J. C. Hummelen, S. J. van der Molen, Observation of quantum interference in molecular charge transport. *Nat. Nanotechnol.* **7**, 305–309 (2012). doi: 10.1038/nnano.2012.37
9. J. Gu, W. Wu, T. Stuyver, D. Danovich, R. Hoffmann, Y. Tsuji, S. Shaik, Cross conjugation in polyenes and related hydrocarbons: what can be learned from valence bond theory about single-molecule conductance? *J. Am. Chem. Soc.* **141**, 6030–6047 (2019). doi: 10.1021/jacs.9b01420
10. Y. Zhao, R. R. Tykwinski, Iterative synthesis and properties of cross-conjugated *iso*-polydiacetylene oligomers. *J. Am. Chem. Soc.* **121**, 458–459 (1999). doi: 10.1021/ja983288p
11. Y. Zhao, R. McDonald, R. R. Tykwinski, Synthesis and characterization of cross-conjugated polyenynes. *Chem. Commun.* 77–78 (2000) doi: 10.1039/A906900C
12. R. R. Tykwinski, Y. Zhao, Cross-conjugated oligo(enynes). *Synlett* **12**, 1939–1953 (2002). doi: 10.1055/s-2002-35578
13. Y. Zhao, A. D. Slepkov, C. O. Akoto, R. McDonald, F. A. Hegmann, R. R. Tykwinski, Synthesis, structure, and nonlinear optical properties of cross-conjugated perphenylated *iso*-polydiacetylenes. *Chem. Eur. J.* **11**, 321–329 (2005). doi: 10.1002/chem.200400822
14. T. M. Swager, R. H. Grubbs, Synthesis and properties of a novel cross-conjugated conductive polymer precursor: poly(3,4-diisopropylidenecyclobutene). *J. Am. Chem. Soc.* **109**, 894–896 (1987). doi: 10.1021/ja00237a042
15. S. S. H. Mao, T. D. Tilley, Cross-conjugated polymers via condensation of a zirconocene alkynyl(benzyne) derivative generated by thermolysis of $Cp_2ZrMe(C_6H_4C{\equiv}CSiMe_3)$. *J. Organomet. Chem.* **521**, 425–428 (1996). doi: 10.1016/0022-328x(96)06353-x
16. T. M. Londergan, Y. You, M. E. Thompson, W. P. Weber, Ruthenium catalyzed synthesis of cross-conjugated polymers and related hyperbranched materials. copoly(arylene/1,1-vinylene)s. *Macromolecules* **31**, 2784–2788 (1998). doi: 10.1021/ma971711t

17. K. Itami, Y. Ohashi, J.-i. Yoshida, Triarylethene-based extended π-systems: programmable synthesis and photophysical properties. *J. Org. Chem.* **70**, 2778–2792 (2005). doi: 10.1021/jo0477401
18. N. Nishioka, S. Hayashi, T. Koizumi, Palladium(0)-catalyzed synthesis of cross-conjugated polymers: transformation into linear-conjugated polymers through the Diels−Alder reaction. *Angew. Chem. Int. Ed.* **51**, 3682–3685 (2012). doi: 10.1002/ange.201200303
19. G. W. P. van Pruissen, J. Brebels, K. H. Hendriks, M. M. Wienk, R. A. J. Janssen, Effects of cross-conjugation on the optical absorption and frontier orbital levels of donor–acceptor polymers. *Macromolecules* **48**, 2435–2443 (2015). doi: 10.1021/acs.macromol.5b00046
20. K. Jiang, L. Zhang, Y. Zhao, J. Lin, M. Chen, Palladium-catalyzed cross-coupling polymerization: a new access to cross-conjugated polymers with modifiable structure and tunable optical/conductive properties. *Macromolecules* **51**, 9662–9668 (2018). doi: 10.1021/acs.macromol.8b02163
21. Q. Zhou, Y. Gao, Y. Xiao, L. Yu, Z. Fu, Z. Li, J. Wang, Palladium-catalyzed carbene coupling of N-tosylhydrazones and arylbromides to synthesize cross-conjugated polymers. *Polym. Chem.* **10**, 569–573 (2019). doi: 10.1039/C8PY01529E
22. H. Hopf, The dendralenes-a neglected group of highly unsaturated hydrocarbons. *Angew. Chem. Int. Ed. Engl.* **23**, 948–959 (1984). doi: 10.1002/anie.198409481
23. M. S. Sherburn, Preparation and synthetic value of π-bond-rich branched hydrocarbons. *Acc. Chem. Res.* **48**, 1961–1970 (2015). doi: 10.1021/acs.accounts.5b00242
24. M. F. Saglam, T. Fallon, M. N. Paddon-Row, M. S. Sherburn, Discovery and computational rationalization of diminishing alternation in [n]dendralenes. *J. Am. Chem. Soc.* **138**, 1022−1032 (2016). doi: 10.1021/jacs.5b11889
25. M. Chen, C. D. Knox, M. C. Madhusudhanan, T. H. Tugwell, C. Liu, P. Liu, G. Dong, Stereospecific alkenylidene homologation of organoboronates by S_NV reaction. *Nature* (2024). doi: 10.1038/s41586-024-07579-7
26. B. Wu, H.-Z. Su, Z.-Y. Wang, Z.-D. Yu, H.-L. Sun, F. Yang, J.-H. Dou, R. Zhu, Copper-catalyzed formal dehydration polymerization of propargylic alcohols via cumulene intermediates. *J. Am. Chem. Soc.* **144**, 4315–4320 (2022). doi: 10.1021/jacs.2c00599
27. H.-Z. Su, B. Wu, J. Wang, R. Zhu, Copper-catalyzed C(3+1) copolymerization of propargyl carbonates and aryldiazomethanes. *Giant* **13**, 100139 (2023). doi: 10.1016/j.giant.2023.100139
28. Z.-L. Wang, R. Zhu, Regioselective condensation polymerization of propargylic electrophiles enabled by catalytic element-cupration. *J. Am. Chem. Soc.* (2024). doi: 10.1021/jacs.4c05524
29. R. P. Johnson, Strained cyclic cumulenes. *Chem. Rev.* **89**, 1111–1124 (1989). doi: 10.1021/cr00095a009
30. W. C. Shakespeare, R. P. Johnson, 1,2,3-Cyclohexatriene and cyclohexen-3-yne: two newhighly strained C_6H_6 isomers. *J. Am. Chem. Soc.* **112**, 8578–8579 (1990). doi: 10.1021/ja00179a050
31. A. V. Kelleghan, A. S. Bulger, D. C. Witkowski, N. K. Garg, Strain-promoted reactions of 1,2,3-cyclohexatriene and its derivatives. *Nature* **618**, 748–755 (2023). doi: 10.1038/s41586-023-06075-8
32. M. Sakura, S. Ando, A. Hattori, K. Saito, Reaction of cyclohexa-1,2,3-triene with N,α-diphenylnitrone: formation of seven-membered cyclic amines via piradone derivatives. *Heterocycles* **51**, 547–556 (1999). doi: 10.1002/chin.199929159

33. R. O. Angus, M. N. Janakiraman, R. A. Jacobson, R. P. Johnson, Small-ring cyclic cumulenes: synthesis and x-ray crystal structure of bis(triphenylphosphine)chloro(.eta.2-1,2,3-cyclononatriene)rhodium. *Organometallics* **6**, 1909–1912 (1987). doi: 10.1021/om00152a013
34. Y. Mizukoshi, K. Mikami, M. Uchiyama, Aryne polymerization enabling straightforward synthesis of elusive poly(*ortho*-arylene)s. *J. Am. Chem. Soc.* **137**, 74–77 (2015). doi: 10.1021/ja5112207
35. M. F. Saglam, A. R. Alborzi, A. D. Payne, A. C. Willis, M. N. Paddon-Row, M. S. Sherburn, Synthesis and Diels–Alder reactivity of substituted [4]dendralenes. *J. Org. Chem.* **81**, 1461–1475 (2016). doi: 10.1021/acs.joc.5b02583
36. M. Bürger, N. Ehrhardt, T. Barber, L. T. Ball, J. C. Namyslo, P. G. Jones, D. B. Werz, Phosphine-catalyzed aryne oligomerization: direct access to *α,ω*-bisfunctionalized oligo(*ortho*-arylenes). *J. Am. Chem. Soc.* **143**, 16796−16803 (2021). doi: 10.1021/jacs.1c08689
37. C. S. Hartley, Folding of *ortho*-phenylenes. *Acc. Chem. Res.* **49**, 646−654 (2016). doi: 10.1021/acs.accounts.6b00038
38. S. Ando, E. Ohta, A. Kosaka, D. Hashizume, H. Koshino, T. Fukushima, T. Aida, Remarkable effects of terminal groups and solvents on helical folding of *o*-phenylene oligomers. *J. Am. Chem. Soc.* **134**, 11084−11087 (2012). doi: 10.1021/ja303117z
39. S. Wang, X. Feng, Z. Zhao, J. Zhang, X. Wan, Reversible *cis-cisoid* to *cis-transoid* helical structure transition in poly(3,5-disubstituted phenylacetylene)s. *Macromolecules* **49**, 8407–8417 (2016). doi: 10.1021/acs.macromol.6b02116
40. L. Yuan, Y. Huang, X. Chen, Y. Gao, X. Ma, Z. Wang, Y. Hu, J. He, C. Han, J. Li, Z. Li, X.Weng, R. Huang, Y. Cui, L. Li, W. Hu, Vitamin C stabilizes n-type organic semiconductors. *Nat. Mater.* (2024). doi: 10.1038/s41563-024-01933-w
41. S. Maruo, O. Nakamura, S. Kawata, Three-dimensional microfabrication with two-photon-absorbed. *Opt. Lett.* **22**, 132–134 (1997). doi: 10.1364/ol.22.000132
42. S. O'Halloran, A. Pandit, A. Heise, A. Kellett, Two-photon polymerization: fundamentals, materials, and chemical modification strategies. *Adv. Sci.* **10**, 2204072 (2023). doi: 10.1002/advs.202204072
43. M. Pawlicki, H. A. Collins, R. G. Denning, H. L. Anderson, Two-photon absorption and the design of two-photon dyes. *Angew. Chem. Int. Ed.* **48**, 3244 – 3266 (2009). 10.1002/anie.200805257
44. M. Totzeck, W. Ulrich, A. Göhnermeier, W. Kaiser, Pushing deep ultraviolet lithography to its limits. *Nat. Photon.* **1**, 629–631 (2007). doi: 10.1038/nphoton.2007.218
45. T. Liu, P. Tao, X. Wang, H. Wang, M. He, Q. Wang, H. Cui, J. Wang, Y. Tang, J. Tang, N. Huang, C. Kuang, H. Xu, X. He, Ultrahigh-printing-speed photoresists for additive manufacturing. *Nat. Nanotechnol.* **19**, 51–57 (2024). doi: 10.1038/s41565-023-01517-w

Acknowledgments:

Funding: This work was supported by Natural Science Foundation of China (223B2102, 22350006, 22222101). **Author contributions**: Z.Y.W. and R.Z. conceived the concept. R.Z., Y.Q.Z., Z.Y.W. designed the project and analyzed data. Z.Y.W., Y.Z.X. and J.Y.L. performed compound synthesis, polymer preparation and characterizations. Z.C. performed femtosecond laser lithography. Z.Y.W. performed DFT calculations. R.Z. and Y.Q.Z. supervised the project. Z.Y.W. and R.Z. wrote the original draft. All authors jointly revised the manuscript. We thank Prof. Zhongze Gu, Dr. Xiaojiang Liu, Dr. Xin Zhou, Mr. Guozhen Wang from the State Key Laboratory of Digital Medical Engineering at Southeast University, China for their help and discussion in two-photon lithography. We thank Dr. Shumu Li (Institute of Chemistry, Chinese Academy of Sciences) for assistance with MALDI-TOF mass spectroscopy. **Competing interests**: The authors declare no competing interests. **Data and materials availability**: All data supporting the findings of this study are presented in the main text or supplementary materials.

Supplementary Materials

Materials and Methods

Supplementary Text

Figs. S1 to S77

Tables S1 to S4

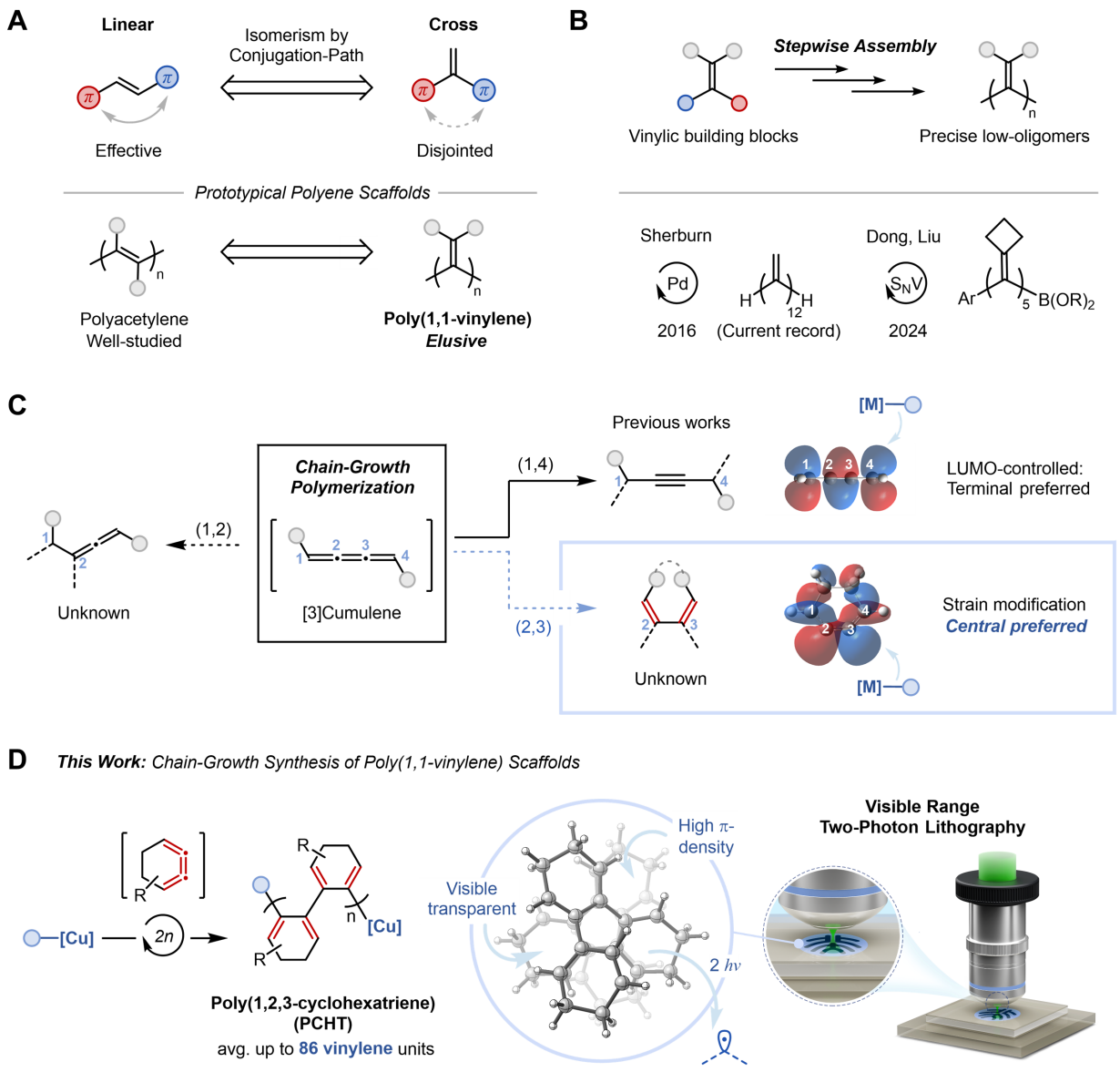

Fig. 1. Challenges in accessing cross-conjugated scaffolds and overview of this work. A. Distinction between linear- and cross-conjugation, and corresponding prototypical polymer scaffolds. **B.** Step-growth methods towards oligo(1,1-vinylene) structures. **C.** Three possible regiochemical outcomes of the chain-growth polymerization of [3]cumulenes. A streamlined synthesis of poly(1,1-vinylene) structures could be enabled by strain-induced 2,3-polymerization. **D.** This work: organocopper-mediated chain-growth synthesis of extensively cross-conjugated polyene frameworks, which enables visible-range two-photon lithography with high resolution.

A

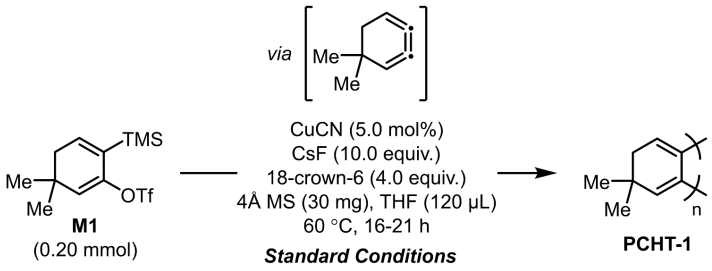

Entry	Deviation from "*Standard Conditions*"	Yield (%)	$M_{n,GPC}$ (kDa)	DP	$Đ$
1	None	65	3.0	29	1.9
2	Without CuCN	—	—	—	—
3	2.5 mol% CuCN	30	4.3	40	1.6
4	Cu≡TIPS instead of CuCN	59	1.5	14	2.9
5	$^{n}Bu_2Cu(CN)Li_2$ instead of CuCN	67	1.9	18	1.4
6	Mesitylcopper instead of CuCN	50	2.0	19	3.0
7	$[Pd(allyl)Cl]_2$ instead of CuCN	7	0.9	9	1.2
8	With 5 mol% PCy_3	43	1.0	10	1.7
9	4.0 equiv. CsF and 2.0 equiv. 18-crown-6	58	1.3	12	2.2
10	$^{n}Bu_4NOTf$ instead of 18-crown-6	33	1.0	10	1.2
11	0.8 mL THF instead of 120 µL	31	1.5	14	1.3
12	Toluene instead of THF	53	1.3	12	1.7
13	1,4-Dioxane instead of THF	52	1.2	11	1.6
14	Without 4Å MS	33	2.3	22	2.6

B

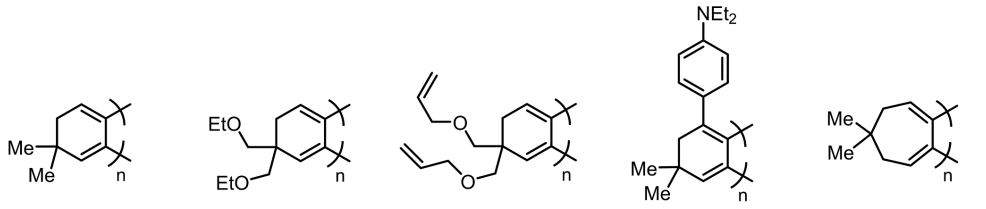

PCHT-1, 65% yield
M_n = 3.0 kDa
$Đ$ = 1.9
DP = 29

PCHT-2, 66% yield
M_n = 6.6 kDa
$Đ$ = 1.3
DP = 34

PCHT-3, 41% yield
M_n = 5.0 kDa
$Đ$ = 1.5
DP = 23

PCHT-4, 78% yield
M_n = 1.8 kDa
$Đ$ = 1.4
DP = 7

PCHPT, 59% yield
M_n = 4.8 kDa
$Đ$ = 1.6
DP = 40

Fig. 2. Cu(I)-mediated 2,3-polymerization of strained [3]cumulenes. A. Selected optimizations. Yields refer to isolated **PCHT-1**, which was purified by precipitation in MeOH/H_2O. $M_{n,GPC}$ and $Đ$ were determined by gel permeation chromatography (GPC) in THF relative to polystyrene standards. DP (degree of polymerization) was estimated by $M_{n,GPC}$. MS = molecular sieve. **B.** Monomer scope.

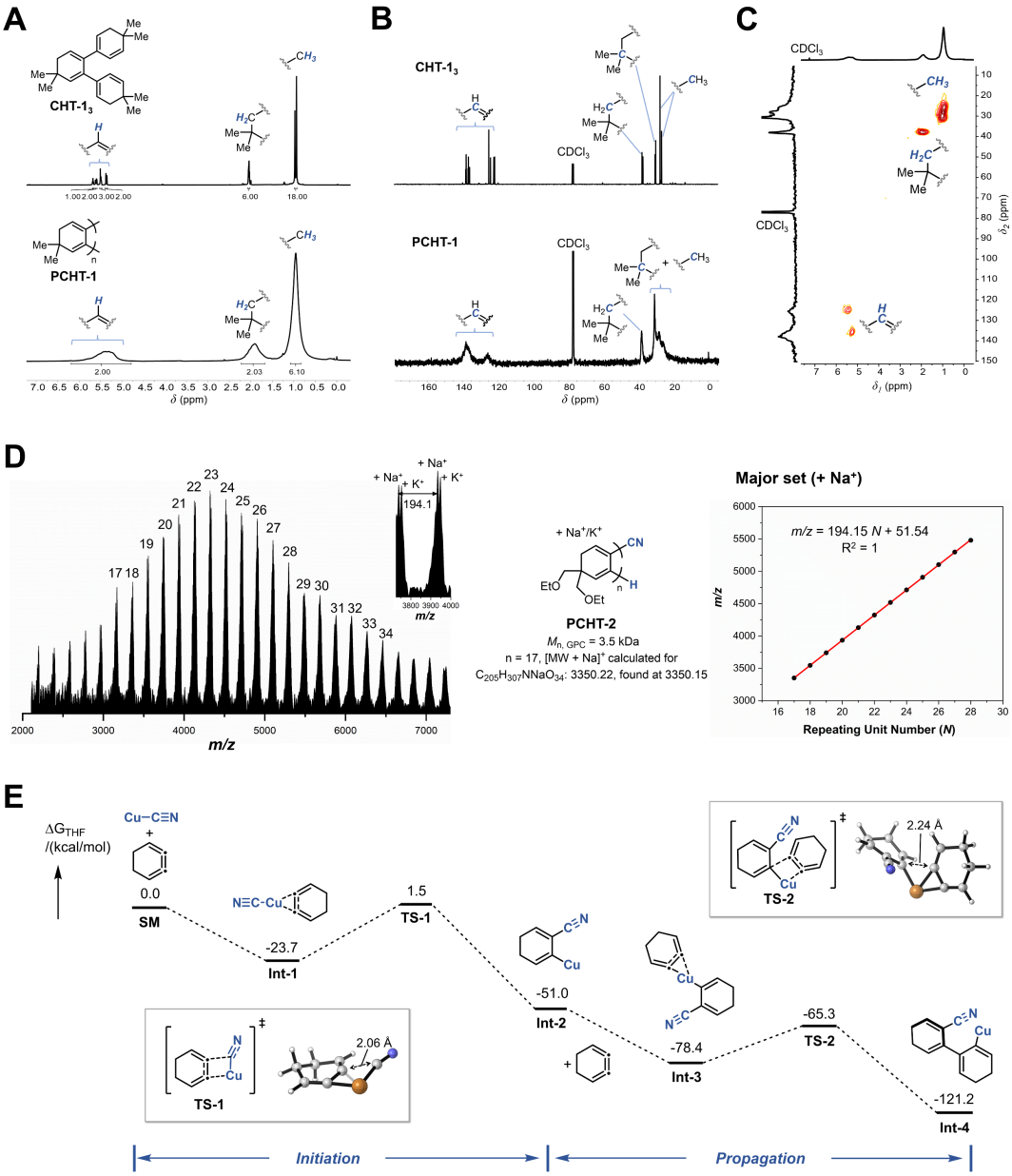

Fig. 3. Structure elucidation of PCHT and computational studies. A.B. Stacked ^{1}H and ^{13}C NMR spectra of **PCHT-1** and **CHT-1$_3$**. **C.** HSQC spectrum of **PCHT-1**. **D.** MADLI-TOF analysis of a sample of **PCHT-2** ($M_{n,GPC}$ = 3.5 kDa). **E.** DFT calculated free energy profile of the 2,3-polymerization pathway. Computed at the SMD(THF)/M06-L-D3/def2-TZVP-LANL2DZ (Cu)//SMD(THF)/B3LYP-D3(BJ)/6-31+G(d,p)-SDD(Cu) level. Side groups were omitted.

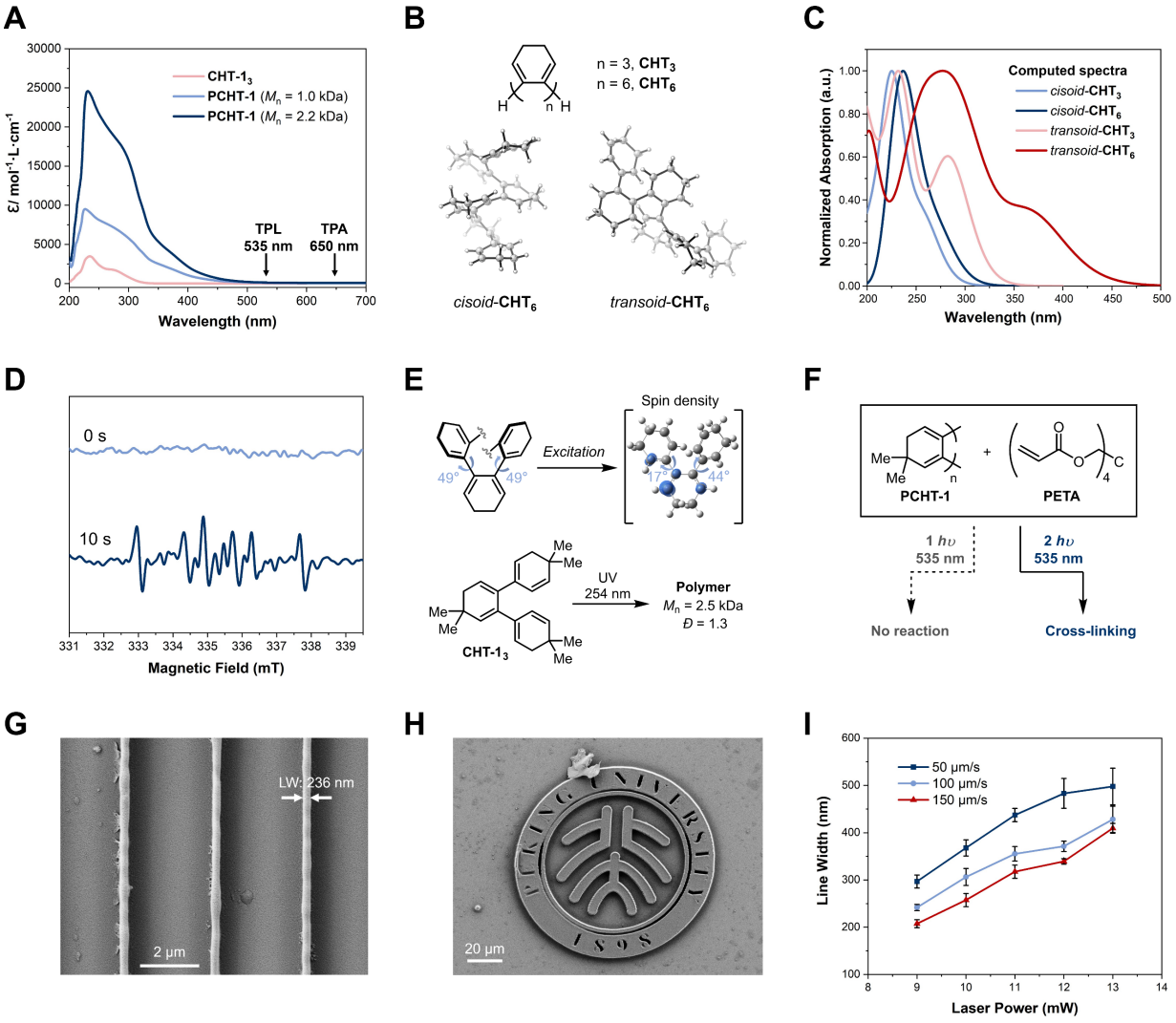

Fig. 4. Optical and photochemical properties of PCHT-1 and application in two-photon lithography. A. UV-Vis absorption spectra of **CHT-1$_3$** and **PCHT-1** ($M_{n,GPC}$ = 1.0 and 2.2 kDa). **B.** Optimized 3D structures for *cisoid*- and *transoid*-conformers of hexamer **CHT$_6$**. **C.** TD-DFT computed UV-Vis spectra of *cisoid*- and *transoid*-oligo(1,2,3-cyclohexatriene)s of varying lengths. **D.** Spin-trapping experiment. A solution of **PCHT-1** in THF was irradiated by a 365 nm LED in the presence of DMPO (10.0 equiv.) and sodium ascorbate at r.t., which was monitored by EPR spectroscopy (g = 2.0059, A_N = 13.2 G, A_H^{β} = 19.6 G). **E.** Analysis of the excited state structure of **CHT$_3$** and photo-induced polymerization of **CHT-1$_3$**. **F.** A photoresist containing **PCHT-1** in

PETA (pentaerythritol tetraacrylate) responded to 535 nm femtosecond laser but not 535 nm continuous-wave laser. **G.** An SEM image of parallel line arrays fabricated by a 535 nm femtosecond laser at a printing speed of 250 μm/s and laser power of 10.0 mW. Scale bar, 2 μm. **H.** An SEM image of an embossed pattern of the logo of Peking University at a printing speed of 100 μm/s and laser power of 12.5 mW. Scale bar, 20 μm. **I.** Influence of laser power and printing speed on line width. (error bars represent mean ± SD for five independent measurements, SD = standard deviation).